THE JOURNAL OF BIOLOGICAL CHEMISTRY VOL. 287, NO. 47, pp. 39887–39897, November 16, 2012

Blood Vessel Epicardial Substance (Bves) Regulates Epidermal Tight Junction Integrity through Atypical Protein Kinase C*[S]

Received for publication, April 15, 2012, and in revised form, September 5, 2012 Published, JBC Papers in Press, September 27, 2012, DOI 10.1074/jbc.M112.372078

Yu-Ching Wu[‡], Chia-Yang Liu[§], Yau-Hung Chen[¶], Ruei-Feng Chen[‡], Chang-Jen Huang[**], and I-Jong Wang[‡‡1]

From the [‡]Institute of Zoology, College of Life Science, National Taiwan University, Taipei 10673, Taiwan, the [§]Department of Ophthalmology, Graduate Program of Neuroscience, University of Cincinnati College of Medicine, Cincinnati, Ohio 45267-0838, the [¶]Graduate Institute of Life Sciences, Tamkang University, Tamsui 25137, Taiwan, the [**]Institute of Biological Chemistry, Academia Sinica, Taipei 115, Taiwan, and the [‡‡]Department of Ophthalmology, National Taiwan University Hospital, Taipei 10002, Taiwan

Background: The regulatory mechanisms of Bves in tight junction integrity is not fully understood.
Results: Both aPKC and Bves are indispensable for claudin expression in cell membrane of zebrafish keratinocytes.
Conclusion: Bves works in coordination with aPKC to regulate claudin formation and stability.
Significance: Bves may play an important role in regulating tight junction integrity through aPKC.

Bves is widely observed in the cell junction of the skin, epicardium, intestine, and cornea of both developmental embryos and mature adults. However, it is not clear how Bves confers its role in intercellular adhesion. Here, we identified the zebrafish *bves* (zBves) and found that the epidermal barrier function could be disrupted after knockdown of Bves, and these zBves morphants were sensitive to osmotic stress. A loss of zBves would affect the partitioning defective protein (PAR) junctional complex identified by the rescue experiment with *tjp-2*/ZO-2 or the PAR complex (*par-3*, *par-6*, and *prkci*/atypical (a)PKC) mRNAs, in which the survival rate of embryos increased 11, 24, 25, and 28%, respectively, after injection with junctional components; the *tjp-2* and aPKC mRNA-rescued embryos also had 24 and 45% decreases in the defective rate. Immunofluorescent studies demonstrated that the aggregation of aPKC around the cell junctions had disintegrated in zBves morphants. However, the expression and assembly of zBves were not influenced by aPKC-MO. These results indicate that a loss of zBves affects the proteins involved in the pathway of the PAR junctional complex, especially aPKC, and both aPKC and Bves are indispensable to claudin expression.

Recent studies have made great progress in revealing the molecular basis of tight junction (TJ)[2] signaling complexes (which modulate cell polarity) by identifying numerous polarity proteins and the interactions between them (1, 2). One set of polarity proteins includes the atypical protein kinase C-partitioning defective protein (aPKC-PAR) system, which is evolutionarily conserved and plays a critical role in the establishment of cell polarity in different organisms and cell types (3, 4).

The aPKC-PAR system contains PAR-3, PAR-6, aPKC, and the small GTPase Cdc42 (5). Among these components, PAR-3 is the first vertebrate homologue of a PAR protein. PAR-3 is called ASIP (atypical PKC isotype-specific interacting protein) in a rat and is identified as an aPKC-interacting protein (6). ASIP co-localizes with aPKC at TJs in epithelial cells, and the overexpression of a dominant-negative mutant of aPKC results in mislocalization of ASIP and other TJ components, as well as the disruption of the barrier function and epithelial cell polarity (3). Aono and Hirai (7) and Suzuki *et al.* (8) found that aPKC could regulate TJ assembly and/or maintenance by phosphorylating claudin and occludin. Furthermore, a direct interaction between junctional adhesion molecule and PAR-3 suggests that junctional adhesion molecule plays a role in anchoring the aPKC·PAR complex to the TJ (9, 10). These findings illustrate that the ASIP/PAR-3·PAR-6·PKC complex plays a central role in the formation and maintenance of TJs in vertebrate epithelial cells, but the detailed molecular mechanisms whereby these proteins control and regulate epithelial polarity are still unclear.

The *bves* gene encodes a membrane protein, Bves, localized to sites of cell-cell contact, pointing to a possible role in cell adhesion or cell-to-cell interactions (11, 12). Previous *in vitro* studies have shown that Bves co-localizes with the components of TJs, particularly ZO-1 and occludin, in corneal epithelial cell lines and in adult mouse small intestine epithelium (13). The GST pulldown experiments reveal an association between the Bves C terminus and the multimolecular complex containing ZO-1 and that the knockdown of Bves disrupts TJ integrity (13). However, Bves-null mice were not observed to have any overt phenotypes, except for the delayed regeneration of skeletal muscle after cardiotoxin injury (14). Therefore, the function of Bves in terms of epithelial integrity and polarity has not been documented *in vivo*. In this study, we isolated the zebrafish *bves*

* This work was supported in part by National Science Council Grants 983112B002040, 993112B002029, and 992314B002039MY3 and by National Taiwan University Hospital Grant 98S-1105.
[S] This article contains supplemental Figs. S1–S4 and Table S1.
[1] To whom correspondence should be addressed: Dept. of Ophthalmology, National Taiwan University Hospital, Chug-Shan South Rd., Taipei 100, Taiwan. Tel.: 886-2-23123456 (Ext. 65192); Fax: 886-2-23934420; E-mail: ijong@ms8.hinet.net.
[2] The abbreviations used are: TJ, tight junction; aPKC, atypical PKC; MO, morpholino oligonucleotide; dpf, day post-fertilization; hpf, hour post-fertilization; Bves, blood vessel epicardial substance; zBves, zebrafish Bves; PAR, partitioning defective protein.

gene (z*bves*) and found that knockdown of zBves could arrest zebrafish development at the end stage of gastrulation and cause epidermal and pericardial edema. Furthermore, our results show that zBves could associate with the polarity protein, aPKC, to regulate the integrity of TJs by recruiting or tethering the signaling complex, consisting of ASIP/PAR-3, PAR-6, Rac-1/Cdc42, and aPKC, to the TJ proteins.

EXPERIMENTAL PROCEDURES

Zebrafish Line—The standard AB strain was established according to procedures described in Westerfield (15). We used zebrafish over 3 months old as experimental materials. They were easily maintained in aquaria heated to 28.5 °C. All animal protocols used in this study were approved by the Institutional Animal Care and Use Committee of the College of Medicine, National Taiwan University, Taipei, Taiwan.

RT-PCR—The mRNAs were extracted from zebrafish embryos by the TRIzol™ reagent (Invitrogen). Reverse transcription was performed at 42 °C for 30 min, and cDNAs were amplified in a PCR mixture containing gene-specific primers with 35 cycles of denaturation (94 °C for 1 min), annealing (55 °C for 1 min), and elongation (72 °C for 1 min) by the PTC-100 Programmable Thermal Controller (MJ Research, Waltham, MA).

Morpholino Knockdown and Rescue—The following antisense morpholino oligonucleotides (MOs) were purchased from GeneTools (Philomath, OR): a z*bves* translation blocking morpholino (ATGmo, 5′-GATGTTGTGTTGGACATTCTGAGGC-3′) and a z*bves* splice inhibition morpholino (splice MO, 5′-AGAGCAGCCTGAAAGACAATAAAGA-3′). A standard control MO (Cmo, 5′-CCTCTTACCTCAGTTACAATTTATA-3′) with no target in zebrafish (GeneTools) was used as control. Zebrafish embryos at the one- or two-cell stages were chosen to be injected. Because a remarkable phenotype with a low mortality was observed at 2 ng of ATGmo and 4 ng of splice MO, we used these concentrations in subsequent experiments.

For rescue experiments, the mRNAs of z*bves*, *tjp-2* of junctional components, *par-6*, aPKC, *crb1* of junctional complexes, and *cdc42* and *pak-1* of Rho-GTPase were generated *in vitro* after their the open reading frames were cloned into the pGEM-T vector (Promega, Madison, WI). Two predicted aPKC phosphorylation sites in the popeye domain were designed to change serine 174 and serine 260 to alanine (S174A and S260A). The point mutations S174A and S260A were generated by PCR-based site-directed mutagenesis. Mutations were introduced into the pGEMT-zebrafish Bves cDNA construct by replacement of a restriction fragment with synthetic DNA duplexes containing the required codon changes at position 174 or 260. For S174A, the specific mutation was T520G, and for S260A, it was AG778GC. Two truncations of zBves cDNA, 1–306 and 1–366 (amino acids 1–102 and 1–122), lacking its cytoplasmic domain were also designed to perform rescue experiments based on the same pGEM-T vector (Promega). The plasmids were linearized and translated *in vitro* using mMESSAGE mMACHINE (Ambion, Austin, TX). Embryos were co-injected with *bves* ATGmo or splice MO and ~100–200 pg of these above mRNAs for rescue of MO-induced phenotypes.

Polyclonal Anti-zBves Antibody Production—An oligopeptide with the sequence of IDSPEFRSTQMNRGE, corresponding to the *Popeye* domain deduced from z*BVES* cDNA (Transcript ID, ENSDART00000081418 provided in the public domain by European Molecular Biology Laboratory, Cambridge, UK) was synthesized and coupled to a maleimide-activated carrier protein, KLH. The KLH-conjugated peptide was then used to raise antiserum in rabbit. To purify the anti-z*bves* antibody further, the IDSPEFRSTQMNRGE oligopeptide was immobilized by covalent reaction with iodoacetyl groups on gel (Sulfolink; Pierce). The rabbit antiserum was loaded onto a peptide-conjugated gel column, according to the manufacturer's instruction. Fractions containing purified anti-zBves antibody were pooled and concentrated.

Immunoprecipitation and Immunoblots—To extract embryonic proteins, the embryos at the stage we needed were homogenized in RIPA buffer containing protease inhibitor (Roche Applied Science). Immunoprecipitation was performed by using the Catch and Release version 2.0 reversible immunoprecipitation system (Upstate Biotechnology, Inc., Lake Placid, NY) according to the manufacturer's protocol. The immunoprecipitates or protein extracts (15 μg) with sample buffer were loaded and electrophoresed at 80 V through an SDS-10% polyacrylamide denaturing gel. Separated proteins were electrotransferred to nitrocellulose, and the immunoblot was processed. The immunoblots were incubated with affinity-purified anti-zBves (1:2000) or anti-β-actin polyclonal antibodies (1:500, Anaspec, Fremont, CA) and detected using the ECL system (Millipore, Billerica, MA). The expression of β-actin was used as a control to confirm that an equivalent amount of protein extract was loaded in each lane.

Whole-mount Immunofluorescence—For immunofluorescence detection of proteins on whole-mount embryos, staged embryos were fixed in 4% paraformaldehyde at 4 °C overnight. Afterward, these embryos were washed in PBS, 0.1% Triton X-100 (PT) for 30 min at RT and then blocked in PT, 5% BSA at 4 °C overnight. The embryos were incubated with the following primary antibodies in blocking buffer at 4 °C overnight: affinity-purified anti-zBves (1:500), anti-ZO-1 (1:200, Zymed Laboratories Inc.), anti-E-cadherin (1:200, BD Biosciences), and anti-PKCζ (1:200, Santa Cruz Biotechnology, Santa Cruz, CA). Embryos were washed in PT, 1% BSA, and then appropriate secondary antibodies (*i.e.* Alexa 488 1:200, Invitrogen) were added for 2 h at room temperature. Samples were washed, and images were acquired by using confocal microscopy (LSM510 Meta, Zeiss, Thornwood, NY).

In Situ Hybridization—Plasmids containing (pGEMT) cDNAs were linearized, and antisense mRNA was transcribed by SP6 RNA polymerase (New England Biolabs) in the presence of digoxigenin-UTP (Roche Applied Science). Embryos were fixed with 4% paraformaldehyde and hybridized with a digoxigenin-labeled RNA probe in a hybridization buffer. They were then incubated with anti-digoxigenin antibody conjugated with alkaline phosphate and stained with 4-nitro blue tetrazolium chloride and 5-bromo-4-chloro-3-indolyl-phosphate. Whole-mount embryos were cleaned in 100% methanol, placed in 100% glycerol, and evaluated with a difference contrast microscope (DMR, Leica, Wetzlar, Germany) *In situ* hybridization of

whole-mount zebrafish was performed essentially as described previously (16).

Electron Microscopy—At 1–3 dpf, the controls and the z*bves* ATGmo-injected embryos were immersed in a fixative solution containing 1.5% glutaraldehyde and 1.5% paraformaldehyde in 0.1 M cacodylate buffer (pH 7.4) for 2 h at room temperature. After a wash in 0.1 M cacodylate buffer, the samples were post-fixed in 0.2% osmium tetroxide in 0.1 M cacodylate buffer for 16–18 h. The samples were then rinsed in the buffer, dehydrated in a graded series of ethanol, and embedded in Epon 812; 1-m sections were then observed after toluidine blue staining. Thin sections were contrasted with uranyl acetate and lead citrate. Grids were observed by the transmission electron microscopy (Hitachi H-7500, Tokyo, Japan).

Biotin Permeability—Zebrafish embryos were collected at 1 dpf, dechorionated, and exposed to 1 mg/ml SNHS-biotin (Thermo Scientific, Waltham, MA) in PBS for 30 min at 4 °C. The embryos were then washed in PBS with 100 mM glycine, immediately fixed in 4% paraformaldehyde for 1 h at room temperature, embedded in agar, and immersed in 30% sucrose before cryo-sectioning. Sections were incubated with Alexa-488-labeled streptavidin (Invitrogen) and observed under a confocal microscope, and digital photographs were acquired using the same settings and exposure times for each slide.

Osmotic Sensitivity—At 6-hpf, embryos were transferred to the following media: 1 mosM, 80 mosM (45 mM ocean salt), 160 mosM (90 mM ocean salt), and 310 mosM (157 mM ocean salt) solutions. The osmolarity of each solution was less than the estimated physiological osmolarity of zebrafish (230–300 mosM), except for the 310 mosM medium. Mortality was assessed at 1 dpf. Experiments were performed in triplicate and subjected to *t* test analysis to establish statistical significance. To correlate the mortality with the *bves* morphant phenotype, the number of surviving morphants was counted after 1 dpf, and two-way analysis of variance was performed to establish statistical significance.

Reversal of Edema—To determine whether MOs disrupt the water permeability barrier, the osmotic force that drives water into the fish was removed by adding mannitol (Sigma). At 2 dpf, the z*bves* morphants and controls were divided into two groups, which were maintained continuously in tank water (~1 mosM) and isotonic 250 mM mannitol (~250 mosM), respectively. The experiments were designed to test the ability of mannitol to reduce pre-existing edema, and mortality and morphology were determined at 3 and 4 dpf for both the control and morphant embryos. Experiments were performed in triplicate and subjected to *t* tests to establish statistical significance.

RESULTS

Temporal and Spatial Expressions of zBves in Developing Zebrafish Embryos—The gene and protein structures of z*bves* were characterized and isolated (Fig. 1 and supplemental Fig. S1). By RT-PCR and *in situ* hybridization analyses, z*bves* mRNA appeared from the 1-hpf stage to adult fish (Fig. 2, *A–E*). At later stages, z*bves* was expressed in the cells of the envelope layer during gastrulation (5–10 hpf) (Fig. 2, *C*, *H*, and *I*) and in epidermis, brain, heart, and eye during organogenesis (10–72 hpf) (Fig. 2, *D* and *J*). The zebrafish Bves protein, analyzed as a 40-kDa protein (Fig. 2*F*), was detected in the cytoplasm of the envelope layer cells, as early as the appearance of the *bves* mRNA, around 1 hpf (Fig. 2, *G–I′*). However, Bves was detected in the periphery of cells at 12 hpf (Fig. 2, *J* and *J′*). A high expression in the skin was observed (Fig. 2*Q*). To corroborate its localization, whole-mount double stainings of zBves were performed, together with E-cadherin (marker for adhesion junction), ZO-1 (marker for TJ), and F-actin (marker for cytoskeleton). The merged *z* axis and E-cadherin data shows that the zBves, adjacent to the plasma membrane, appears more predominantly in the apical layer than the E-cadherin (Fig. 2*M*). In terms of ZO-1, zBves was expressed in the same layer but further into the cytoplasm than the ZO-1 (Fig. 2*N*). However, the double staining with F-actin reveals that the zBves was co-localized with F-actin (Fig. 2*O*). This result strongly suggests that zBves may impact TJs because of its location on the cytoskeleton.

Effects of zBves Knockdown on Embryonic Development—To investigate the dosage effect of the morpholino-induced phenotypes, two kinds of the z*bves* MOs, ATGmo and splice MO, were designed (Fig. 1*B*). The morphological alterations were classified into wild type-like and severe defects (Fig. 3, *H* and *I*). The severity of the phenotypes was dose-dependent; to induce the same phenotype, the concentration of splice MOs required was twice that of the ATGmo. Co-injection of z*bves* MOs and the z*bves* mRNA revealed a significant reduction in the number of morphants, showing that the MO-induced phenotypes can be rescued specifically by z*bves* mRNAs (supplemental Table S1). At 20 hpf, zBves knockdown embryos exhibited multiple defects, including shortened body length, deformed body figure, brain malformation with a small eye field, incomplete somite segmentation without ordered V-shaped trunk somites, irregular muscle arrangement, failed tail extension, a ratio of yolk extension/yolk ball less than ½, and an enlarged pericardium (Fig. 3, *G–I*). Western blots showed that expression was almost completely eliminated in z*bves* MO-injected samples (supplemental Fig. S2*A*).

A possible role of zBves in the early developmental process was studied from yolk plug closure stage to the segmentation stages. At 8 hpf (late-gastrulation), both MO-injected embryos exhibited a bulging yolk plug in the vegetal region, as well as delayed epiboly (Fig. 3, *B* and *C*). This suggests that zBves is needed for epibolic morphogenesis, where extensive cell movement drives the cells over the egg surface and deep cells undergo gastrulation. Consequently, an extended body length, an enlarged pericardium, and a deformed tail bud (when compared with the control embryos) (Fig. 3*D*) were found in the 11-hpf knockdown embryos (Fig. 3, *E* and *F*). The abnormalities in these embryos, as defined above, were worse at 20 hpf. Microscopic analysis showed that separation between epidermal cells (Fig. 3*J–L′*), as well as increased space between the epidermis and muscle (Fig. 3, *M–O* and supplemental Fig. S2*B*), was also noted in *z*Bves knockdown embryos, relative to the control embryos.

Epidermal Barrier Function Was Compromised in zBves Morphants—Since incorporation of zBves into cell junctions could be found as early as the 12-hpf stage in the epidermis (Fig. 2*J′*), we attributed the aforementioned phenotypes to the compromised skin barrier function in the z*bves* morphants. During

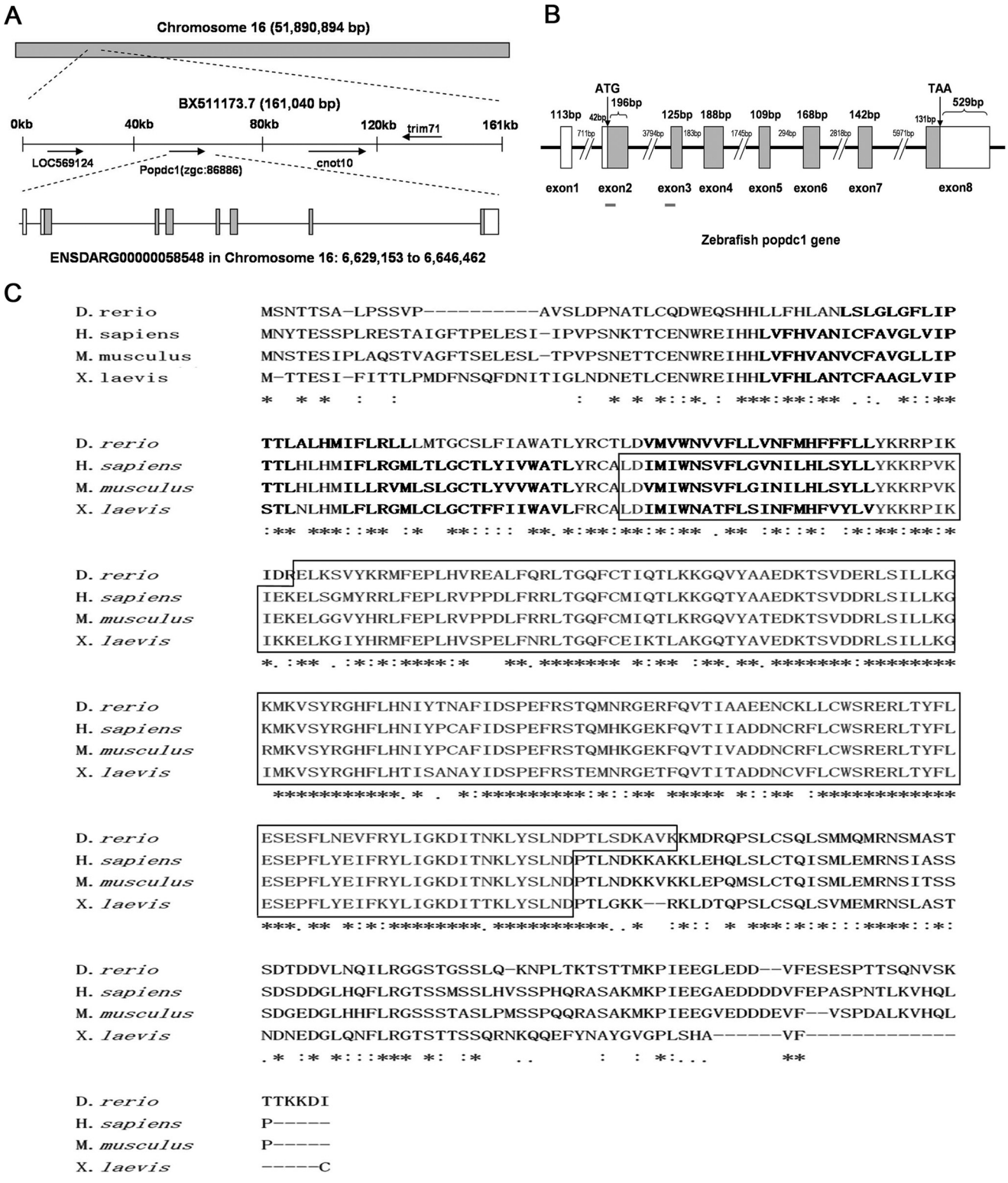

FIGURE 1. **Identification of zebrafish *bves*.** *A,* genetic map of the zebrafish *bves* locus and the exon/intron structure of the *bves* transcript were constructed through blasting the *BVES* cDNA sequence to the genome databases of the Ensembl website. The *bves* (zgc:86887) was ENSDARG00000058548 in chromosome 16, 6,629,153 to 6,646,462. *B,* schematic diagram showing the organization of the *zbves* gene. Regions to which ATG and splice morpholinos were bound are indicated by *lines*. *C,* sequence comparison between *bves* homologues. The complete amino acid sequences of *Homo sapiens* (human), *Mus musculus* (mouse), *Xenopus laevis* (*Xenopus*), and *Danio rerio* (zebrafish) *bves* were aligned. Sequence identities between Bves proteins of different species were compared. Single, fully conserved residues were marked by *asterisks*. The *colon* and *dot* indicated amino acid conservation of strong and weak groups, respectively. Transmembrane domains are shown as *boldface letters* and conserved popeye domains are *boxed*.

the process of morphological observation, we found that z*bves* MO-injected (ATGmo and splice MOs) embryos were not tolerant of highly viscous solution (*i.e.* 3% methylcellulose, which was often used as a medium for photographing zebrafish embryos). The knockdown embryos displayed body distortion and skin ruptures within 5 min of transfer to methylcel-

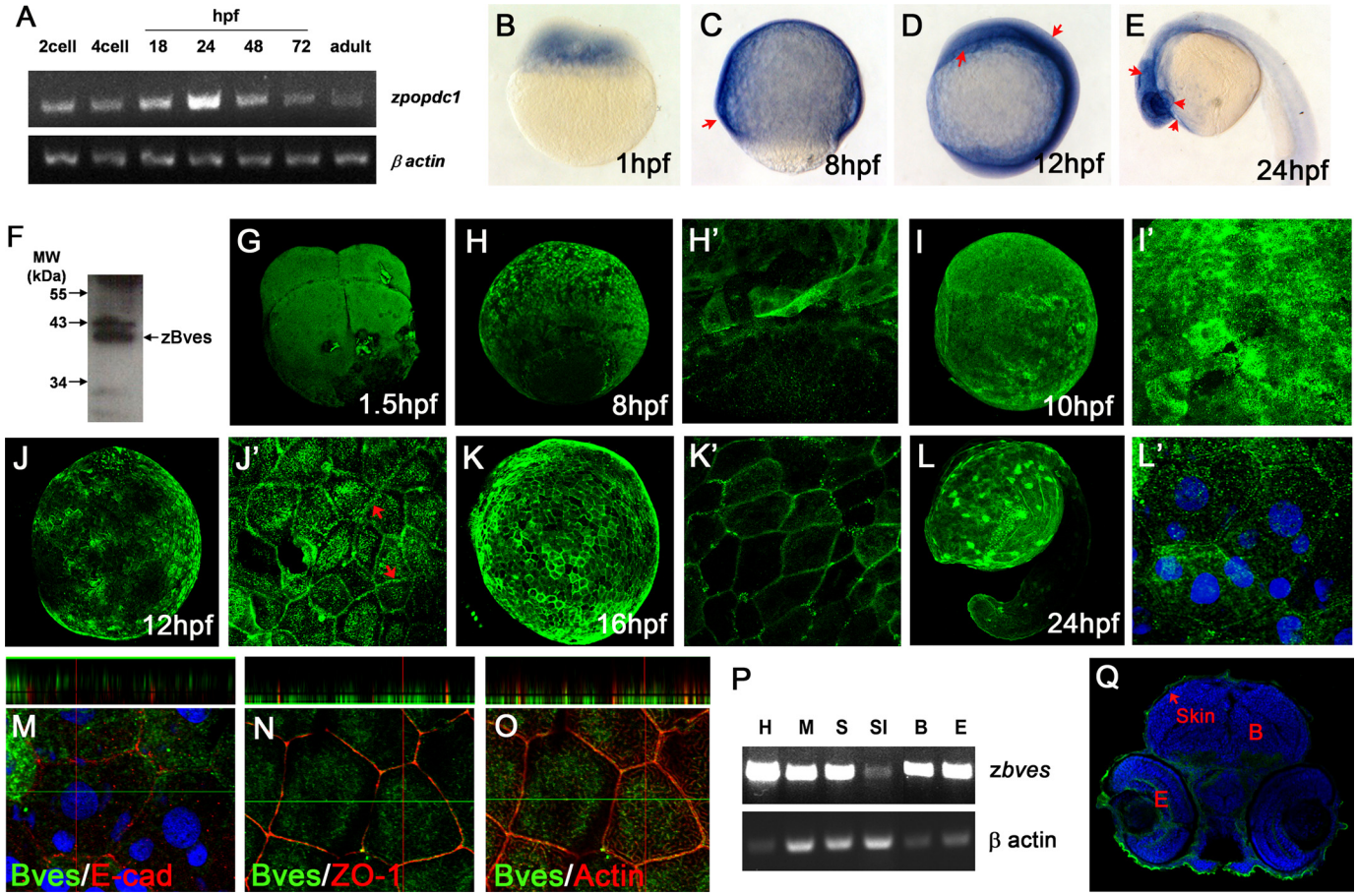

FIGURE 2. **Temporal and spatial expressions of zBves in developing zebrafish embryos.** *A, zbves* expression by RT-PCR analyses. The amplified *zbves* PCR product could be found from 1 hpf to adult. *B–E,* whole-mount *in situ* hybridization analyses of *zbves* mRNA in early zebrafish larvae. *zbves* mRNA was detected as early as 1-hpf embryo. In older zebrafish larvae (24 hpf), the hybridization signals were detected in the eyes and whole body (*arrows*). *F,* ~40-kDa band was visualized by Western blot with anti-zBves antibody. *G–L′,* immunofluorescence staining pattern of zBves protein was found in 1.5 hpf as early as the mRNA appears. Magnification in surface is shown (*H′*, *I′*, *J′*, *K′*, and *L′*). Note that Bves protein emerged in the periphery of cells in the EVL at the 12-hpf stage (*arrow*). *Scale bars,* 100 μm. *M–O,* apical/lateral distribution of zBves in the epidermis of zebrafish embryos. The merged and *z* axis data revealed that zBves at the cell membrane appeared more predominantly than E-cadherin protein in the apical layer (*M*) and was expressed in the same layer of ZO-1 (*N*) and F-actin (*O*). *P,* tissue distribution of *zbves* by RT-PCR. The PCR product could be found not only in the heart but also in other tissues. Actin was used as the internal control. *Q,* as the RT-PCR data, zBves immunofluorescence staining patterns on the frozen section of 3-dpf zebrafish were expressed in epidermis and eye. *Scale bars,* 20 μm. *H,* heart; *M,* muscle; *S,* skin; *SI*, small intestine; *B,* brain; *E,* eye.

lulose, whereas the control MO (Cmo)-injected embryos remained intact under the same condition (Fig. 4). This difference implies that zBves is involved in the formation of the epidermal barrier.

To elucidate the function of zBves in the epidermis, the skins of *zbves* MO-injected embryos were subjected to morphological analysis with TEM at 1–3 dpf (Fig. 5, *A–F*). The space below the TJ between the cells increased at the 3-dpf stage in *zbves* MO-injected embryos, when compared with Cmo-injected embryos (Fig. 5, *C* and *F*). In addition, the length of the TJ in the *zbves* MO-injected embryos at the 2- and 3-dpf stages was significantly shorter than that of the Cmo-injected embryo (supplemental Fig. S3). In addition, paracellular diffusion barriers in the epidermis of *zbves* morphants were also estimated according to the permeability of sulfo-NHS-biotin, a small (~440 Da) membrane-impermeable tracer often used to assess the intactness of the epithelial barrier in these fish. In controls, no staining in the epidermis layer was observed (Fig. 5, *G* and *H*). In contrast, 83 and 67% of embryos injected with ATGmo and Splice MO, respectively, show fluorescent signals resulting from biotin infiltration. A striking accumulation of biotin in the segmental cavity between the epidermis and the muscle cells was found in morphants (Fig. 5, *I* and *J*).

zBves Morphants Were Sensitive to Osmotic Stress—Given the importance of TJs in controlling paracellular permeability, and the paramount role of zBves in epidermal barrier function, we further investigated the effect of osmotic stress on *zbves* morphants. Morphologically, the ATGmo-injected embryos became shriveled in a high salt solution (Fig. 6*A*). Likewise, the survival rate of ATGmo-injected embryos in high salt conditions was much lower than the control embryos or the rescued embryos co-injected with *zbves* mRNA (Fig. 6*B*).

Due to the hypo-osmotic environment of tank water, a defect in the epidermal barrier function is expected to result in passive water influx into the body. Furthermore, if this influx exceeds the volume that can be cleared by the kidneys, the fluid will accumulate under the skin, or in the pericardium, and cause edema. To determine whether the zBves knockdown disrupted the water permeability barrier, different osmotic forces, which

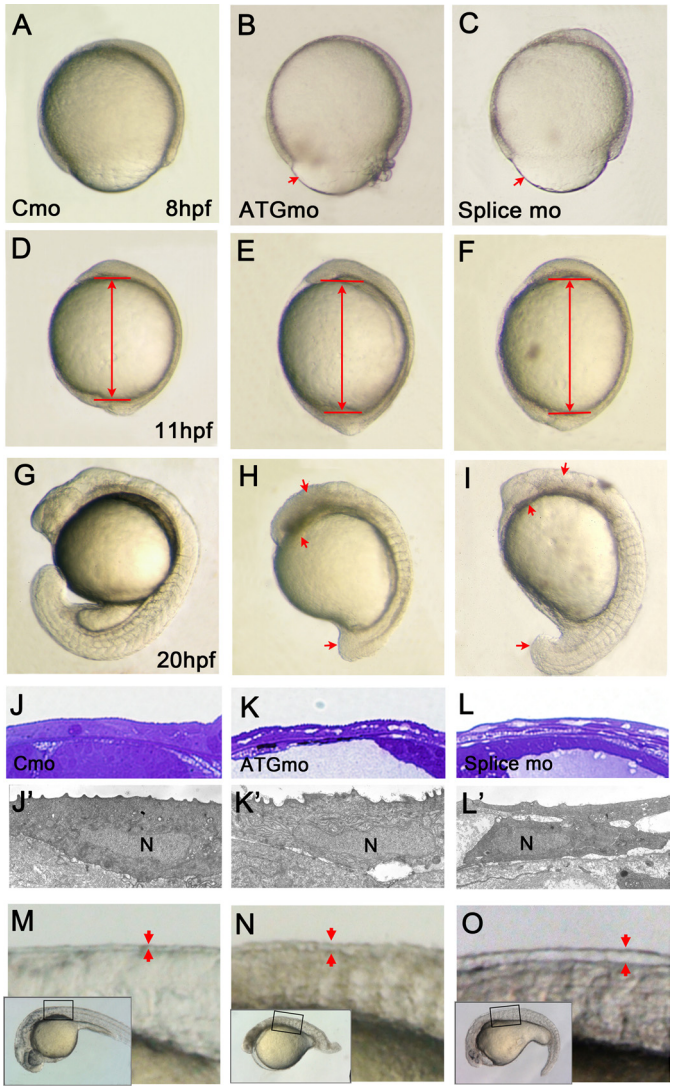

FIGURE 3. **Characterization of the *zbves* morpholino phenotype.** Zebrafish embryos were injected with Cmo, ATGmo, or splice MO against zBves. *A–I,* both *zbves* MO-injected embryos present the same phenotypes. At 8 hpf, morphants had a cell migration defect on embryonic surface (*A–C*). An increased embryo length appeared on 11-hpf morphants (*D--F*), and then a deformed body shape with multiple defects arose at 20 hpf (*G–I*). *J–L′,* histological studies in control and *zbves* MO-injected embryos at 3 dpf. The semithin Epon sections were observed after toluidine blue staining. Note that epidermal cells in zBves knockdown embryos revealed a loose connection (*K′* and *L′*). *M–O,* magnifying observation in zebrafish epidermis. By 1 dpf, pericardial and epidermis edemas were increased (*N* and *O*).

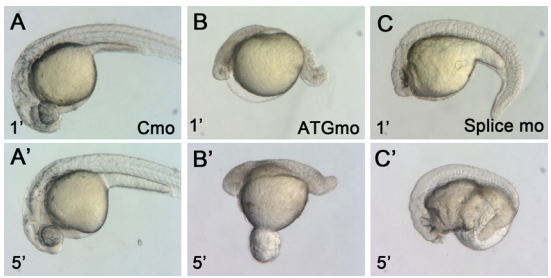

FIGURE 4. **zBves knockdown embryos were fragile in hyperosmotic medium, 3% methylcellulose.** *A–C′,* embryos injected with control MO, ATGmo, and splice MO were transferred to 3% methylcellulose solution. The ruptures of skin of morphants were seen immediately in 5 min in this hyperosmotic solution (compare *B′* and *C′* to *B* and *C*), whereas control MO-injected embryos still maintained normal body shape (*A* and *A′*).

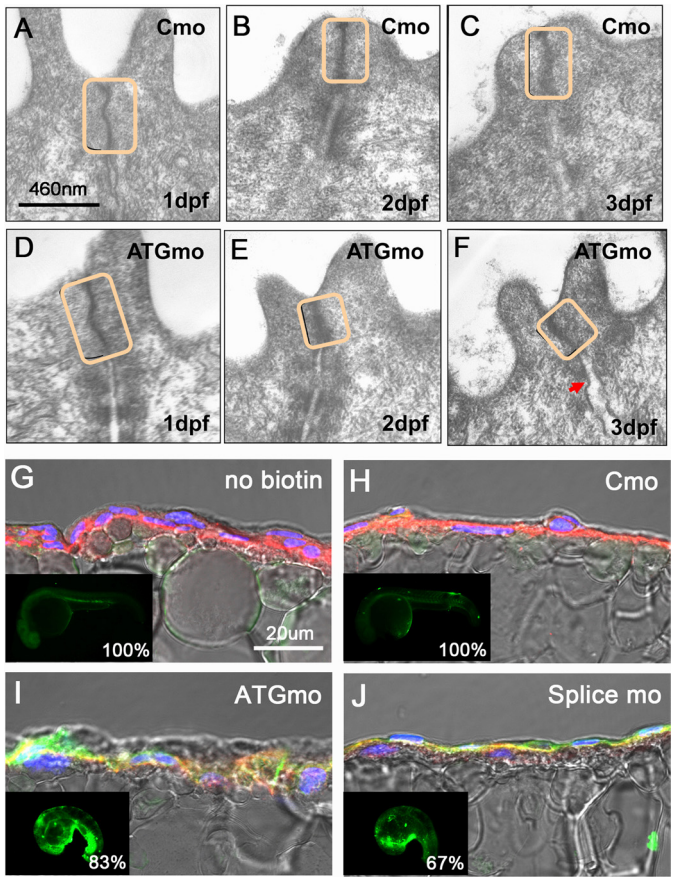

FIGURE 5. **Epidermis defects in zBves knockdown embryos.** *A–F,* ultrastructure of the epidermis under the electron microscope was emphasized on attached sites between the cells at 1–3 dpf. Compared with the control group, the zBves knockdown embryos had shorter TJs and an obvious separation of the adhesion junction (*F*). *G–J,* biotin was treated to observe a leak in the epidermis of 1 dpf morphants. In the negative control, without biotin (*G*) and Cmo-injected embryos (*H*), no biotin diffusion was detected. A significant accumulation of biotin was observed between epidermal cells in MO-injected embryos (*I* and *J*) The *insets* and percentages of fluorescent infiltration are shown in the *lower left corners* ($n = 12$).

drive water into the fish, were applied to the control and the ATGmo-injected fish. Higher osmotic forces led to a higher mortality rate in the zBves knockdown embryos than in the control embryos, indicating a weakened epidermal layer in the zBves knockdown embryos. However, these could be rescued by co-injection with z*bves* mRNA (Fig. 6*B*). When fish embryos treated with ATGmo were placed in a 250 mM mannitol solution, a significant reduction in embryo edema, without altering the mortality rate, was observed (Fig. 6, *C* and *D*). The restoration of edema with a 250 mM mannitol solution was even more striking in the skin and muscle than that rescued with water (supplemental Fig. S4).

Role of zBves in the Molecular Pathway during Junction Formation or Maintenance—Whole-mount immunofluorescence was performed with embryos injected with Cmo, ATGmo, and ATGmo + z*bves* mRNA at 1 dpf with E-cadherin, ZO-1, and claudin monoclonal antibodies (Fig. 7, *B–S*). Among these cell junction proteins, the claudin expression of ATGmo-injected embryos was significantly decreased when compared with the control or rescued embryos (Fig. 7*I*), whereas there was no difference in E-cadherin and ZO-1 expression between the knock-

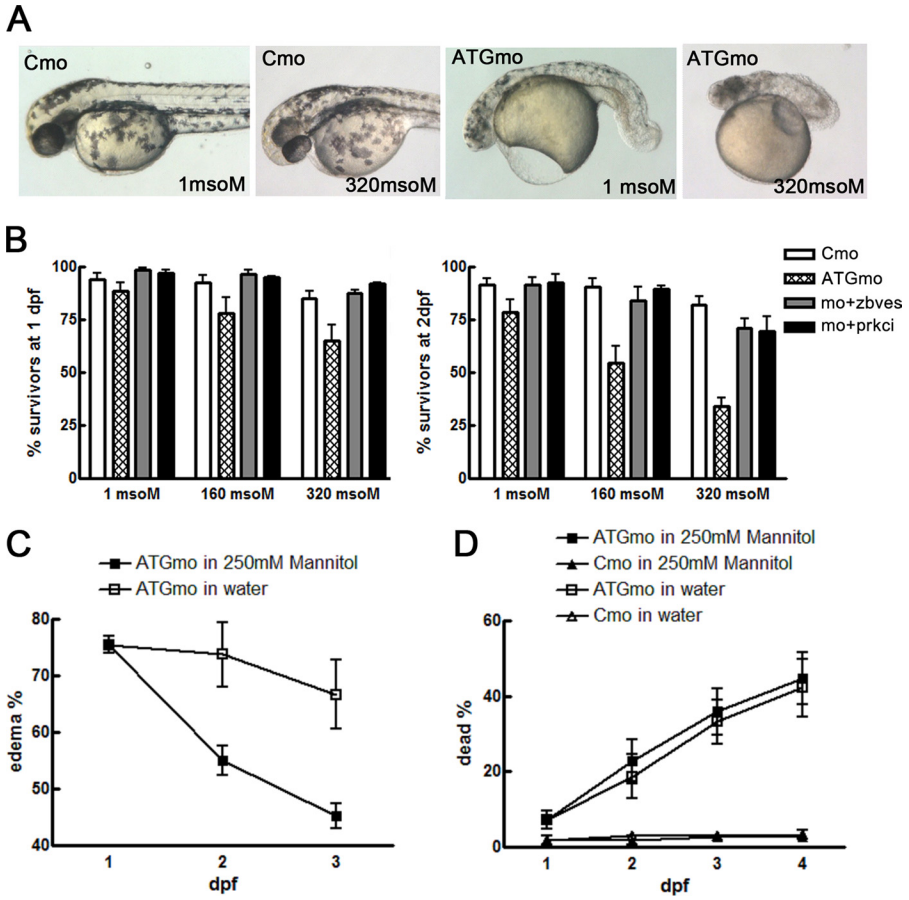

FIGURE 6. **zBves knockdown embryos lose the complete barrier to maintain osmotic homeostasis.** *A, zbves* morphants are sensitive to osmotic stress. Compared with control embryos, zBves knockdown embryos revealed significant shrinkage at 2 dpf. *B,* ability of morphants to survive high osmotic conditions were counted at 1 and 2 dpf and were significantly reduced compared with control or *zbves* or *aPKC* mRNA rescued embryos. *C,* epidermal edema of zBves knockdown embryos can be reversed by growing the embryos in a hyperosmotic mannitol solution. If grown in tank water (*open square*), the incidence of edema only slightly decreased, due to individuals that died. However, if *zbves* morphants were grown in 250 mM mannitol (*filled square*), edema incidence dropped significantly. *D,* there was no statistical significance between mortality of controls or morphants in 250 mM mannitol. $n > 40$ per experiment; 4 independent experiments. Two-way analysis of variance; *, $p < 0.01$.

down and the normal or rescued embryos (Fig. 7, *C* and *F*). This result implies that zBves has a role in epidermal barrier function by affecting TJs. As formation and regulation of the TJs would influence the paracellular permeability, we further elucidated its role in these aspects. After injection with junctional components (*tjp-2*/ZO-2) or the PAR complex (*par-3*, *par-6*, and aPKC) mRNAs, the survival rate of embryos increased to 11, 25, 24, and 28%, respectively. The *tjp-2* and aPKC mRNA-rescued embryos also had 24 and 53% decreases in defective rates. Significantly, the survival and normality rate of the aPKC mRNA-rescued embryos was two to three times greater than that of the knockdown embryos (Fig. 7*A*). These results indicate that a loss of zBves affects the proteins involved in the pathway of the PAR junctional complex, especially aPKC, and then further influences the expression of claudin.

To determine the relationship between zBves, aPKC, and claudin *in vivo*, embryos injected with aPKC MO were compared with those injected with z*bves* MO (ATGmo) through whole-mount immunofluorescent staining. Like the z*bves* MO-injected embryos, the disappearance of claudin was observed in aPKC MO-injected embryos (Fig. 7*K*). In z*bves* MO-injected embryos, the aggregation of aPKC around the cell junctions was disorganized (Fig. 7*M*). However, when aPKC was knocked down by aPKC MO, the expression and assembly of zBves were not influenced (Fig. 7*S*). These results suggest that Bves may play a role in aPKC maintenance around the cell membrane and further regulate the claudin in TJs.

Effect of zBves Knockdown on aPKC and Claudin Assembly—To confirm the findings mentioned above, untreated and z*bves* MO-injected embryos were collected at 2, 6, 10, 12, 18, and 24 hpf; then the membrane and cytosolic fractions of the zBves, aPKC, and claudin proteins were examined separately by Western blot (Fig. 8*A*). In untreated embryos, membrane zBves proteins began appearing at 12 hpf, corresponding to our immunostaining data, although this was significantly decreased in z*bves* MO-injected embryos. Following knockdown of zBves by MO, the amount of aPKC was reduced, and the claudin had disappeared from the membrane; in contrast, the amount of cytosolic aPKC and claudin protein in both the untreated and the z*bves* MO-injected embryos increased during development. These data show that zBves knockdown reduced the expression of aPKC and claudin around the plasma membrane.

In contrast, in aPKC morphants, the level of claudin decreased in the membrane fraction but there was no influence on Bves expression. As zBves morphants were co-in-

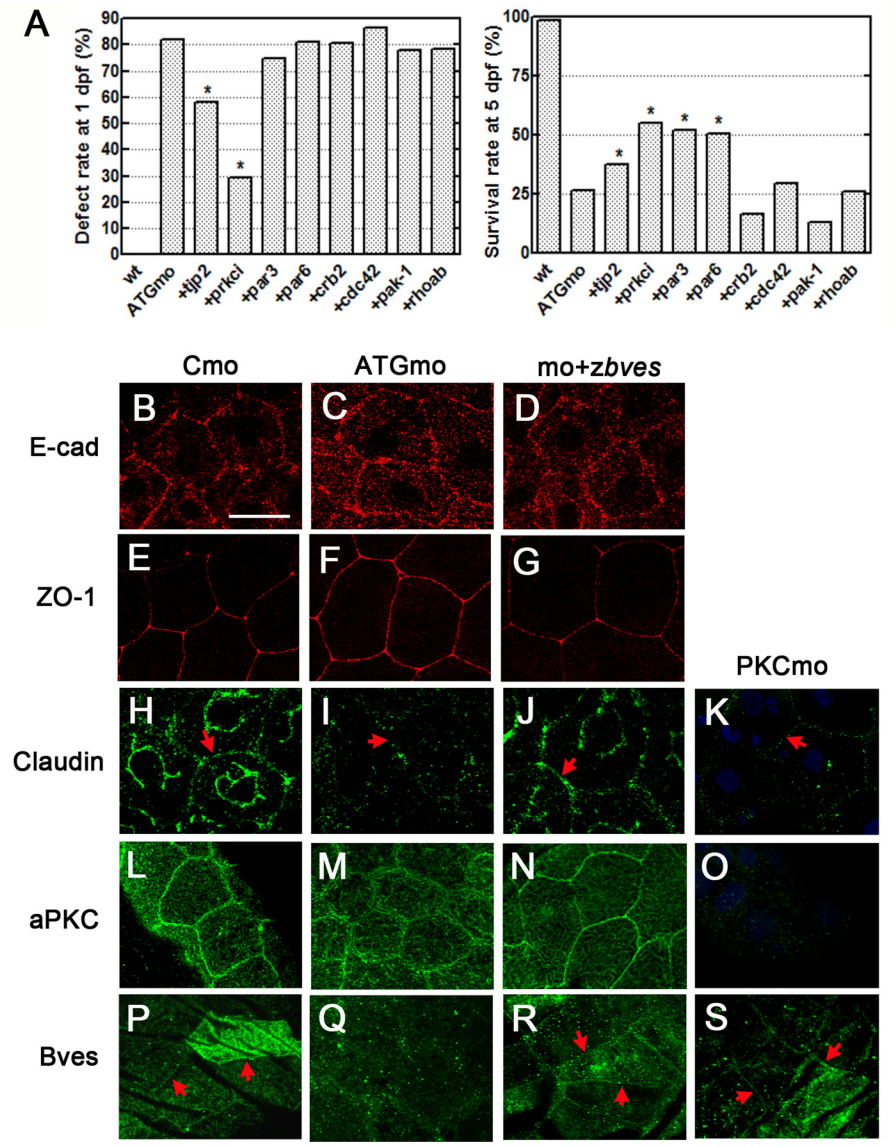

FIGURE 7. **Influence of zBves knockdown on the regulation of the cell junction.** *A,* rescue experiments. The defect and survival rates in the zebrafish embryos co-injected with ATGmo and mRNAs are associated with tight junction formation. Comparing the mRNA rescue group with the knockdown group by χ^2, *, $p < 0.05$. *B–S,* immunofluorescent staining experiment. ATGmo-injected embryos had decreased expression of claudin (*H–K*) and zBves (*P–S*) and lost the condensed pattern of aPKC (*L--O*), whereas there were no changes in E-cadherin (*B–D*) and ZO-1 (*E–G*). Also, *aPKC* MO-injected embryos (*K, O,* and *S*) were used to determine the relation between zBves and the aPKC protein, and they revealed an unaffected pattern in the zBves protein (*S*).

jected aPKC mRNAs, the claudin can be rescued partially (Fig. 8*A*).

Furthermore, immunoprecipitation of claudin and aPKC was compared between the zBves knockdown embryos and the untreated embryos. We found that the amount of aPKC associated with claudin was significantly reduced when zBves was knocked down (Fig. 8*B*). Besides, the level of phosphorylated aPKC was also decreased but could be rescued partially by co-injected aPKC mRNAs. These results indicate that zBves can affect the association between aPKC and claudin.

To investigate the association of zBves with aPKC, co-immunoprecipitation analysis was performed. Whole embryo lysates were immunoblotted with anti-zBves or anti-aPKC antibodies to confirm the expression of these proteins (Fig. 8*C, 1st lane*). When embryo lysates were used for immunoprecipitation in conjunction with anti-zBves and anti-aPKC antibodies, aPKC was found to associate with zBves (Fig. 8*C*, *2nd* and *3rd lanes*). These results reveal that zBves can form a complex with aPKC.

To find the possible interaction site between zBves and aPKC, we re-performed the rescue experiments with two mRNAs (1–306 and 1–366) truncated at the C-terminal Bves cDNAs. Our results show that all truncated Bves mRNAs cannot rescue the development defect of morphants as effective as that of full-length Bves mRNA (Fig. 8*D*). Furthermore, two point mutants of Bves cDNA constructs from two predicted aPKC phosphorylation sites in the popeye domain are designed to change serine 174 and serine 260 to alanine (S174A and S260A). Interestingly, we find that S260A mutant can rescue the defect in morphants as that of full-length Bves mRNA (Fig. 8*D*). However, S174A mutant cannot rescue the developmental defects as that of full-length Bves mRNA. This result implies

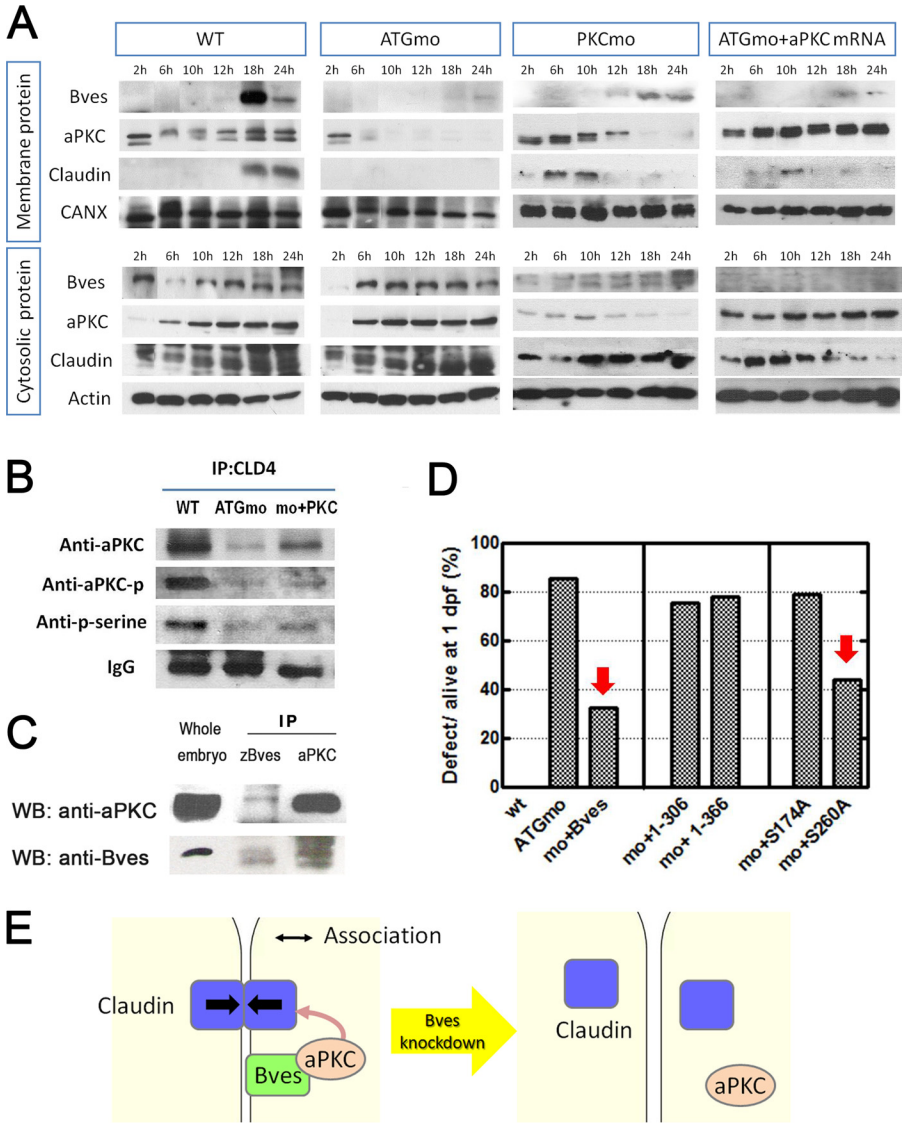

FIGURE 8. **Relationship between Bves, aPKC, and the claudin protein.** *A,* membrane and cytosolic proteins of Bves, aPKC, and claudin were detected separately by Western blotting in developing embryos at 2, 6, 10, 12, 18, and 24 hpf. aPKC and claudin expression in membrane were decreased following Bves disruption by ATGmo. Inhibition of aPKC by PKCmo reduced claudin expression in the membrane but not Bves. Claudin was rescued slightly via overexpression of aPKC by co-injected aPKC mRNA in Bves morphants. *B,* at 18-hpf, claudin was immunoprecipitated (*IP*) to observe the effect of zBves disruption, and the influences on phosphorylation of claudin and aPKC are shown. Bves knockdown decreased the interaction between claudin and aPKC. *C,* immunoprecipitations were adopted to observe the interaction between zBves and aPKC protein. The lysates extracted from 1-dpf embryos were immunoprecipitated with zBves or aPKC antibodies. These immunoprecipitated zBves lysates were used to perform Western blots (*WB*) with aPKC antibody and vice versa. zBves and aPKC proteins were detected in both immunoprecipitated lysates. The interaction between zBves and aPKC is shown. *D,* two C-terminal truncated Bves mRNA were co-injected with Bves ATGmo and failed to rescue the defect in morphants. To find the critical site in Bves C terminus, two point mutants (S174A and S260A) were developed. S260A mutant could rescue the defect in morphants as that of full-length Bves mRNA but S174A could not. *E,* a suggested model in which Bves acts as an adaptor to anchor aPKC from the PAR complex at the plasma membrane. This association makes aPKC close to TJ components, claudin, and further regulates TJ formation. The integrity of TJ formation totally influences the establishment and maintenance of barrier function. Consequently, the linkage of claudin cannot be maintained and/or formed as Bves disappear in membrane.

that Ser-174 may play a crucial role in the association between aPKC and Bves.

DISCUSSION

Through knockdown experiments, cell movement defects appeared in *zbves* morphants during the gastrulation period (Fig. 3, *B* and *C*); the cells that covered the yolk surface of the morphants could not involve, converge, and extend in an ordinary way, resulting in a bulging yolk plug. This finding was also noted in the study by Ripley *et al.*(17), in which Bves knockdowns influenced corneal epithelial cell migration. Furthermore, it is of interest to note that the zBves protein could be detected at the cell periphery in the immunofluorescent stainings at the end of gastrulation (Fig. 2*J′*), and zBves knockdown perturbed the orientation of embryonic epithelia in late gastrulation, through inappropriate cell-cell interactions, leading to severely defective phenotypes (Fig. 3, *H* and *I*). When zBves knockdown embryos were subjected to an acute hypertonic medium (3% methyl cellulose), ruptures in the epidermis appeared, and the body shape of the embryo was immediately distorted (Fig. 4). These findings suggest that zBves in the epidermal layer acts as a regulator in maintaining the barrier func-

tion in an aquatic environment. Consequently, the subepidermal and epidermal edemas of the morphants were the result of a hypotonic environment, and the rupture of morphants in the hypertonic medium could be observed in, and was confirmed by, biotin and osmotic stress experiments, which showed that biotin permeation through the morphant epidermis increased mortality, and shrinking of the morphant accompanied higher osmotic stress.

In the epidermis of 1 dpf zebrafish, the zBves protein adjacent to the membrane was mainly expressed near the TJs and co-localized with F-actin, and a decrease of claudin expression was found in the zBves knockdown embryos (Fig. 7*F*). Therefore, we speculate that zBves influences the barrier function of the epidermis by regulating the TJ function, possibly via claudin. The results of rescue experiments with mRNAs of Cdc42, Pak1, and Rhoab (for small GTPase), PAR-3, PAR-6, and aPKC (for PAR complex), and Crb2 (for Crumb complex) show that aPKC expressed the highest efficiency in rescuing the death of morphants (Fig. 7*A*), which was further confirmed by the osmotic stress experiment (Fig. 6*B*). Our data strongly indicate that aPKC may play a pivotal role in mediating zBves epidermal barrier function, which is also supported by previous research, as the aPKC enzyme activity was required for barrier function in previous studies (18, 19).

aPKC is required for the barrier function in the granular layer of keratinocytes, the site of tight junctions, through the association with other proteins such as PAR-6, PAR-3, and Cdc42 (19). Our study further provides evidence for the association of aPKC between zBves and claudin (Fig. 8, *B* and *C*), through the phosphorylation level of claudin and aPKC by zBves (Fig. 8*B*). The aPKC lost its condensed expression pattern surrounding the plasma membrane, as well as its association with claudin in z*bves* knockdown embryos (Figs. 7*M* and 8*B*). In contrast, zBves expression was not affected in aPKC knockdown embryos (Fig. 7*S*). Therefore, we conclude that zBves might play an upstream regulator role, recruiting aPKC to make it stay at adjoining membrane.

Suzuki *et al.* (8) and Aono and Hirai (7) found that aPKC could phosphorylate occludin and claudin-4 at the intracellular domains for TJ formation in Madin-Darby canine kidney and human keratinocytes, respectively. In our study, claudin did not express in the membrane fraction when either Bves or aPKC was absent (Fig. 8*A*). Significant decreases of the claudin were not only found adjacent to the epidermal cell membrane (Fig. 7, *I* and *M*) but also in the phosphorylation levels of claudin and aPKC (Fig. 8*B*) in z*bves* knockdown embryos. This indicates that aPKC cannot be maintained in the plasma membrane, and claudin failed to form during zBves knockdown (Fig. 8*A*). These results imply that zBves may be an upstream regulator that influences the assembly and phosphorylation of the aPKC and claudin proteins. Furthermore, point mutants of Bves mRNA rescue experiments demonstrate that mutation in Ser-174 of Bves, a predicted aPKC phosphorylation site, failed to rescue the development defect in Bves morphants (Fig. 8*D*). We speculated that aPKC could interact with the C terminus of Bves, especially at Ser-174 site.

In conclusion, our results suggest Bves acts as an adaptor to anchor aPKC and PAR complex at the plasma membrane and further influences the phosphorylation level of claudin to regulate TJ formation (Fig. 8*D*). This novel finding demonstrates a relationship between zBves, aPKC, and claudin in TJs, which is important for gaining insight into the mechanism by which barrier function is established and maintained in epidermal epithelia.

Acknowledgments—We thank Carolyn Chuang and Ya-Wen Hsu for their help throughout this study, Dr. Ming S. Chang for critical comments on the manuscript, and the second core laboratory of National Taiwan University Hospital for supplying the space and instruments. We also thank Hui-Chun Kung and Ya-Ling Chen for their help throughout the TEM image study at the Microscope Center of Chang-Gung Memorial Hospital.

REFERENCES

1. Bilder, D. (2001) Cell polarity: squaring the circle. *Curr. Biol.* **11,** R132–R135
2. Yamanaka, T., Horikoshi, Y., Suzuki, A., Sugiyama, Y., Kitamura, K., Maniwa, R., Nagai, Y., Yamashita, A., Hirose, T., Ishikawa, H., and Ohno, S. (2001) PAR-6 regulates aPKC activity in a novel way and mediates cell-cell contact-induced formation of the epithelial junctional complex. *Genes Cells* **6,** 721–731
3. Suzuki, A., Yamanaka, T., Hirose, T., Manabe, N., Mizuno, K., Shimizu, M., Akimoto, K., Izumi, Y., Ohnishi, T., and Ohno, S. (2001) Atypical protein kinase C is involved in the evolutionarily conserved PAR protein complex and plays a critical role in establishing epithelium-specific junctional structures. *J. Cell Biol.* **152,** 1183–1196
4. Wodarz, A., Ramrath, A., Grimm, A., and Knust, E. (2000) *Drosophila* atypical protein kinase C associates with Bazooka and controls polarity of epithelia and neuroblasts. *J. Cell Biol.* **150,** 1361–1374
5. Lin, D., Edwards, A. S., Fawcett, J. P., Mbamalu, G., Scott, J. D., and Pawson, T. (2000) A mammalian PAR-3-PAR-6 complex implicated in Cdc42/Rac1 and aPKC signaling and cell polarity. *Nat. Cell Biol.* **2,** 540–547
6. Izumi, Y., Hirose, T., Tamai, Y., Hirai, S., Nagashima, Y., Fujimoto, T., Tabuse, Y., Kemphues, K. J., and Ohno, S. (1998) An atypical PKC directly associates and colocalizes at the epithelial tight junction with ASIP, a mammalian homologue of *Caenorhabditis elegans* polarity protein PAR-3. *J. Cell Biol.* **143,** 95–106
7. Aono, S., and Hirai, Y. (2008) Phosphorylation of claudin-4 is required for tight junction formation in a human keratinocyte cell line. *Exp. Cell Res.* **314,** 3326–3339
8. Suzuki, T., Elias, B. C., Seth, A., Shen, L., Turner, J. R., Giorgianni, F., Desiderio, D., Guntaka, R., and Rao, R. (2009) PKCη regulates occludin phosphorylation and epithelial tight junction integrity. *Proc. Natl. Acad. Sci. U.S.A.* **106,** 61–66
9. Ebnet, K., Suzuki, A., Horikoshi, Y., Hirose, T., Meyer Zu Brickwedde, M. K., Ohno, S., and Vestweber, D. (2001) The cell polarity protein ASIP/PAR-3 directly associates with junctional adhesion molecule (JAM). *EMBO J.* **20,** 3738–3748
10. Itoh, M., Sasaki, H., Furuse, M., Ozaki, H., Kita, T., and Tsukita, S. (2001) Junctional adhesion molecule (JAM) binds to PAR-3: a possible mechanism for the recruitment of PAR-3 to tight junctions. *J. Cell Biol.* **154,** 491–497
11. Reese, D. E., Zavaljevski, M., Streiff, N. L., and Bader, D. (1999) Bves. A novel gene expressed during coronary blood vessel development. *Dev. Biol.* **209,** 159–171
12. Andrée, B., Hillemann, T., Kessler-Icekson, G., Schmitt-John, T., Jockusch, H., Arnold, H. H., and Brand, T. (2000) Isolation and characterization of the novel popeye gene family expressed in skeletal muscle and heart. *Dev. Biol.* **223,** 371–382
13. Osler, M. E., Chang, M. S., and Bader, D. M. (2005) Bves modulates epithelial integrity through an interaction at the tight junction. *J. Cell Sci.* **118,** 4667–4678
14. Andrée, B., Fleige, A., Arnold, H. H., and Brand, T. (2002) Mouse Pop1 is

required for muscle regeneration in adult skeletal muscle. *Mol. Cell. Biol.* **22,** 1504–1512
15. Westerfield, M. (1995) in *The Zebrafish Book: A Guide for the Laboratory Use of Zebrafish* (*Danio rerio*) (Knight, J, ed) pp. 2–5, University of Oregon Press, University of Oregon, Eugene, OR
16. Thisse, C., and Thisse, B. (2008) High resolution *in situ* hybridization to whole-mount zebrafish embryos. *Nat. Protoc.* **3,** 59–69
17. Ripley, A. N., Chang, M. S., and Bader, D. M. (2004) Bves is expressed in the epithelial components of the retina, lens, and cornea. *Invest. Ophthalmol. Vis. Sci.* **45,** 2475–2483
18. Helfrich, I., Schmitz, A., Zigrino, P., Michels, C., Haase, I., le Bivic, A., Leitges, M., and Niessen, C. M. (2007) Role of aPKC isoforms and their binding partners Par3 and Par6 in epidermal barrier formation. *J. Invest. Dermatol.* **127,** 782–791
19. Denning, M. F. (2007) Tightening the epidermal barrier with atypical PKCs. *J. Invest. Dermatol.* **127,** 742–744